Journal of Hydrology 669 (2026) 135040

Contents lists available at ScienceDirect

Journal of Hydrology

journal homepage: www.elsevier.com/locate/jhydrol

Research papers

Land cover influences microclimate and non-rainfall water inputs in temperate agricultural environment

Jannis Groh [a,b,c,*], Thomas Pütz [b], Daniel Beysens [d,e], Joan Cuxart [f], Nurit Agam [g], Werner Küpper [b], Paul D. Colaizzi [h], Harry Vereecken [b], Horst H. Gerke [c], Wulf Amelung [a,b]

[a] Institute of Crop Science and Resource Conservation – Soil Science and Soil Ecology, University of Bonn, Bonn, Germany
[b] Institute of Bio- and Geoscience (IBG-3, Agrosphere), Forschungszentrum Jülich GmbH, Jülich, Germany
[c] Leibniz Centre for Agricultural Landscape Research (ZALF), Landscape Functioning, Isotope Biogeochemistry and Gasfluxes, Müncheberg, Germany
[d] Physique et Mécanique des Milieux Hétérogènes, CNRS, ESPCI, PSLResearch University, Sorbonne Université, Sorbonne, Paris, France
[e] OPUR, Organisation pour l'Utilisation de la Rosée, 2 rue Verderet, Paris, France
[f] University of the Balearic Islands, Palma, Spain
[g] Blaustein Institutes for Desert Research, Ben-Gurion University of the Negev, Israel
[h] Conservation and Production Research Laboratory, USDA-ARS, Bushland, TX, USA

ARTICLE INFO

This manuscript was handled by Amilcare Porporato, Editor-in-Chief, with the assistance of Rachata Muneepeerakul, Associate Editor

Keywords:
Non-rainfall water
Dew
Fog
Water vapor adsorption
Lysimeter
Ecohydrology
Land cover

ABSTRACT

Non-rainfall water inputs (NRWI) from dew, fog, frost, rime and soil water vapour adsorption (WVA) are key components of the terrestrial water cycle, but their individual contribution to the water budget is unclear due to a lack of suitable methods for identification and quantification. Here, we present a refined method to quantify and partition NRWI using weighing lysimeters. The method's novelty lies in the variables used to determine when dew and frost (leaf-wetness), fog and rime (air visibility) occur. We applied this methodology to grassland and arable land lysimeters and compared it to the established method that relies on relative humidity and estimated dew-point temperature to quantify and partition NRWI.

Our results showed large differences between the refined and established method. The established method predicted larger amounts of dew (55 %) and WVA (2522 %), but no fog. NRWI mostly came from dew. Dew rates per event were generally higher on arable land, but the total amount of dew was larger on grassland due to higher frequency of dew formation. Dew amount differences could be attributed to land cover type, which promoted dew formation in the grassland while the arable ecosystem largely lost water through evapotranspiration (e.g. stomatal conductance, canopy-structure). We conclude that land cover type is a key control for microclimate (surface temperature, relative humidity), which significantly affects dew formation, while effects on fog or WVA are weaker. These effects are better determined by lysimeter assessment with a visibility and leaf-wetness device than by other existing NRWI identification systems.

1. Introduction

In temperate regions, rainfall constitutes the largest fraction of water input (excluding irrigation) to terrestrial ecosystem and is the most decisive parameter of the water cycle. Plant growth and ecosystem productivity are dependent on rainfall in many parts of the world (Knapp et al., 2017), as they are sensitive to changes in water availability (Vargas Zeppetello et al., 2024). As plant growth has strong feedbacks with land–atmosphere exchange processes (Liu et al., 2018; Han et al., 2020; Martins et al., 2021), a precise understanding of atmospheric water inputs and related feedbacks is crucial for comprehending and simulating the functioning of terrestrial ecosystems.

Noteworthy, in many regions of the world, also non-rainfall water inputs (NRWI) contribute water to ecosystems in addition to rain- and snowfall (Wang et al., 2017; Dawson and Goldsmith, 2018). The generation of NRWI comprises various processes; they originate from fog (Li et al., 2018), dew (Kaseke et al., 2012), frost or frozen dew (Groh et al., 2018), rime (Meissner et al., 2007), and soil water vapor adsorption (WVA; Kosmas et al., 1998; Agam and Berliner, 2004). From the meteorological perspective, fog is defined as a cloud that touches the ground and reduces horizontal visibility to less than 1 km (Gultepe et al., 2007). Fog is formed from condensed liquid droplets in the atmosphere, it has a

* Corresponding author at: Institute of Crop Science and Resource Conservation – Soil Science and Soil Ecology, University of Bonn, Bonn, Germany.
E-mail address: jgroh@uni-bonn.de (J. Groh).

https://doi.org/10.1016/j.jhydrol.2026.135040
Received 10 July 2025; Received in revised form 30 November 2025; Accepted 26 January 2026
Available online 31 January 2026

relative humidity of 100 %, so that fog water can be collected through active or passive fog collectors on artificial surfaces (Sträter et al., 2010; Degefie et al., 2015). Dew forms when atmospheric water vapor condenses on a surface whose temperature is equal to or below the dew point temperature. Both dew or frost (temperature below frost point) are also often measured on artificial or natural surfaces, e.g., by leaf wetness sensors (Sibley et al., 2022), dewmeters (Price and Clark, 2014), or weighable lysimeters (Marek et al., 2014; Groh et al., 2018). Compared to fog or dew, WVA occurs when the soil surface is dry enough to form a downward gradient of water vapor concentration and atmospheric water vapor penetrate the soil and adsorb to soil particles (Agam and Berliner, 2004). This NRWI component has mainly been measured using weighable lysimeters (Verhoef et al., 2006; Kohfahl et al., 2019), while more recently attempts have made use of negative latent heat fluxes from eddy covariance and scintillometer measurements (Florentin and Agam, 2017; Paulus et al., 2024). Sometimes, there is also water at the plant surface that originates from water vapor distilled from either the soil (Li et al., 2021) or released through plant guttation (Urbaneja-Bernat et al., 2020). However, unlike dew or fog, these processes do not lead to a net water input, since the water is only redistributed within the ecosystem.

The different NRWI fractions are typically small at the daily scale but they can provide a more continuous source of water as compared to often erratically occurring rainfall, and thus help in maintaining ecosystem functions, e.g., at dry inland regions (Runyan et al., 2019; Kidron et al., 2024b) or wet coastal areas (Chung et al., 2017). There is increasing evidence that dew-derived NRWI contribute considerably to total incoming atmospheric water (i.e., rain, snow), ranging from 5 and 19 % annually at certain locations (Hanisch et al., 2015; Aguirre-Gutiérrez et al., 2019). In dry periods, the dew amounts can even exceed monthly rainfall in temperate climates (e.g., Falkenberg-Germany, Xiao et al., 2009), or annual rainfall amounts in arid regions (e.g., Negev-Israel, Evenari et al., 1982). Variability is high, with a frequency of dew formation for grassland sites ranging from 15 to 95 % in dry (relative humidity < 80 %) to tropical (relative humidity > 90 %) areas, respectively (Ritter et al., 2019). NRWI influence hydrological processes (Hanisch et al., 2015; Yu et al., 2018), energy fluxes (Florentin and Agam, 2017), canopy micro-meteorological conditions (Goldsmith et al., 2013), ecosystem properties such as drought resilience (Fischer et al., 2009; Groh et al., 2018), water use efficiency (Ben-Asher et al., 2010), plant biomass production (Hiatt et al., 2012; Goetz and Price, 2016), microbial activity (McHugh et al., 2015), litter decomposition (Evans et al., 2019), and elemental or nutrient cycling (Gottlieb et al., 2019; Sun et al., 2024). Accurate quantification of NRWI is thus crucial for correctly assessing ecosystem water balances, especially in agricultural landscapes, and thus also for future improving existing crop models.

There are several methods that can quantify NRWI, but only the gravimetric method can measure all types of NRWI and simultaneously determine NRWI for natural surfaces. This is important because, e.g., soil properties and plant surface characteristics influence the formation of NRWI (Malik et al., 2015; Uclés et al., 2016; Saaltink et al., 2020). Sophisticated approaches thus utilize weighable lysimeter data (e.g., Groh et al., 2018; Zhang et al., 2019a; Paulus et al., 2022). Yet, all these methods must rely on specific assumptions when determining and classifying NRWI fractions.

Zhang et al. (2019a), for instance, used relative humidity sensors to detect fog. However, sensed relative humidity observations often do not reach 100 % (Paulus et al., 2022), leading to an underestimation of fog per se. Zhang et al. (2019a) determined dew formation using the criterion that the temperature sensed at the soil surface must be below the dew point temperature. The dew point temperature is calculated 1 m above the surface layer, and can differ substantially from what is measured at the land surface (Kidron et al., 2023) or plant surface. This is because it disregards the typical profiles of increasing humidity and temperature closer to the canopy and soil surface (Ney and Graf, 2018), which leads to an overestimation of dew and WVA. For example, in the case of WVA, if the relative humidity does not reach 100 % during a fog event, the leaf wetness sensor will not detect the typical signal of dew or frost formation. Therefore, the approach would suggest that the leaves are not being rewetted by dew or frost. In this case, any increase in weight would be related to WVA rather than fog. Another important point is that the identification system by Zhang et al. (2019a) introduced a class called 'Others' to describe parts of the uncertainty of the method and to account for water inputs that could not be classified as NRWI, precipitation or dust. In their study of NRWI in a semi-arid region of China (Dingxi; Zhang et al., 2019b), the 'Others' class achieved a value of 23.7 mm y^{-1}, similar to that of dew (25.9 mm y^{-1}) and WVA (26.1 mm y^{-1}). Because of these problems, many field or modeling studies are not considering NRWI as a supplementary water input to rain and snowfall when simulating ecosystem processes. Hence, there is still the need for an improved methodological approach to reduce the uncertainty in the determination and partitioning of NRWI. While weighable lysimeters allow to quantify the NRWI as a total amount, it remains important to distinguish between the different NRWI in order to develop, test, and improve the prediction of dew, fog, frost, rime or WVA at ecosystem level.

This study aims to overcome current limitations in estimating the different fractions and amount of NRWI, and to provide data on integrated observations for both grassland and an arable ecosystem. To do so, in addition to weighable lysimeters, we employed an air visibility measuring device, as well as surface temperature and leaf wetness sensors that allow for the direct determination of each NRWI for different soils and land cover types, but under the same macroclimatic conditions. We compared the results of our methodology to the established method by Zhang et al. (2019a) for NRWI quantification and partitioning. We then determined the influence of land cover form on the formation of different NRWI fractions.

2. Data and methods

2.1. Site description

The study was conducted at the site Selhausen (50°52′7″N, 6°26′58″E), which is part of the Eifel/Lower Rhine Valley Observatory of TERrestrial ENvironmental Observatory in Germany (TERENO, Bogena et al., 2018). The climate in Selhausen is temperate and humid (sub-oceanic or sub-Atlantic), with an average annual air temperature of 10.5°C, potential evapotranspiration for grass as reference (Allen et al., 2006) of 643 mm and annual average precipitation of 718 mm for the period from 1981 to 2010 (Groh et al., 2016).

2.2. Observational data

Eight high-precision weighing lysimeters (UMS, Germany), each cylindrical with an area of 1 m^2 and a soil depth of 1.5 m, which were installed in the context of TERENO-SOILCan (Pütz et al., 2016), were used in this study. The lysimeter was placed on three load cells (Model 3510, Tedea-Huntleigh, US), resulting in a weighing system with a measurement precision of 10 g (equivalent to 0.01 mm water depth) that provides measurements in 1-minute increments. The bottom boundary of the lysimeters is controlled dynamically to keep the soil moisture conditions inside the lysimeter similar to the surrounding soil. This is done via a bi-directional pumping system, including a suction rake in the lysimeter bottom, a weighed water reservoir (UMS, Germany), and tensiometers (TS1, UMS, Germany) installed at 1.4 m soil depth inside the lysimeter and the field (grassland and arable land). This configuration ensures that water flow rates and directions correspond to the conditions in the field (Groh et al., 2016).

The weighable lysimeters contain a total of eight different soils, some of which are from Selhausen (Cutanic Luvisol), and some from other locations in Germany: Bad Läuchstädt (Haplic Chernozem), Dedelow

(Calcic Luvisols), Rollesbroich (Stagnic Cambisols), Sauerbach (Haplic Cambisol), Scheyern (Aeric Epiaquept), and Wüstebach (Stagnic Cambisols). Others are from France Nancy (Technosol). Soils were filled monolithically (i.e., undisturbed), except for the Technosol (packed soil). The type of land surface cover of the eight ecosystems comprises two different natural (Wüstebach, Nancy) and two different extensively managed grasslands (Scheyern, Rollesbroich), as well as four soils cultivated with winter wheat (*Triticum aestivum L.*) during the observation period from 2022-10-01 to 2023–06-30.

The following meteorological variables were measured: air temperature ($T_{air,}$ 2 m, WXT510, Vaisala Oyi, Finland), wind speed (W_s, 2 m, WXT510, Vaisala Oyi, Finland), relative humidity (RH, 2 m, WXT510, Vaisala Oyi, Finland), and air visibility (CS125, 1.5 m, Campbell Scientific, USA). Each lysimeter was equipped with several additional sensors used in this study. The soil heat flux was sensed in each soil using a heat flux plate (G_s, −0.1 m, Hukseflux Thermal Sensors B.V., The Netherlands). Please note that no correction was made for G_s for heat storage above the sensor plate, as this does not affect the general dynamics of G_s and thus would not affect the relationship with the specific NRWI fraction. However, during transition times, G_s in the upper layer and on the surface may have opposite directions. The soil water content (0.1 m) was sensed using time domain reflectometry probes (SWC, CS610, Campbell Scientific, USA) connected to a time-domain reflectometer system (TDR100, Campbell Scientific, USA). The temperature was sensed at different depths with a temperature sensor (T_{soil} (−0.06 m), T_{surf} (0.02 m), T_{intC} (0.15 m), TMS-4, TOMST s.r.o., Czech Republic), and at the canopy surface with an infrared radiometer (T_{canopy}, SI-111-SS, Apogee Instruments, USA). Other sensors were used to determine the leaf wetness (LWS, height variable, METER Group, Germany) and the net radiation (R_n, height variable, Delta OHM S.r.L., Italy). All sensor data was provided with a time resolution of 10-minutes, with exception of leaf wetness and air visibility, which provide data with a greater frequency (1-minute). Information on dust deposition was obtained using a self-made dew collector (weekly samples). This collector opens during night and closes during the day, depending on the hours of daylight, by wiping of the water from a window every morning. The sample is collected under the window. If it rains or there is fog, the outlet valve is activated and diverts the sample water. The dew water samples were then filtered (PORAFIL membrane filter MV 0.45 µm), and the dry mass of the dust input was determined gravimetrically. The sensors of the meteorological station, LWS, and dew collector are shown in the supplementary material (Fig. 1).

2.3. Data processing

The raw 1-minute lysimeter and leachate tank weight data were processed as follows: i) manual and automatic plausibility checks to remove systematic errors and outliers, ii) application of the Adaptive Window and Adaptive Threshold (AWAT) filter routine (Peters et al., 2017) to reduce the effect of noise on the determination of land surface water fluxes (i.e. precipitation, NRWIs, evapotranspiration), and iii) calculation of land surface water flux components. The latter calculation assumes that either evapotranspiration or atmospheric water inputs (i.e., precipitation, NRWIs) can occur during a one-minute time interval (e.g., Schrader et al., 2013; e.g. see Schneider et al., 2021). This means that after correcting for weight changes in the lysimeter caused by water flows at the bottom, any subsequent decrease in lysimeter weight will be related to evapotranspiration, while any increase will be related to atmospheric water inputs. Further information on lysimeter data processing can be found in Schneider et al. (2021). Also, the weather and soil related sensor 10-minute raw data underwent manual and automatic plausibility checks to remove unreliable observations (systematic errors and outliers). More information about the time without data for each lysimeter can be taken from Table S1. Smaller gaps within the time

Fig. 1. Experimental set-up at the site Selhausen (Germany), showing the 24 high-precision weighing lysimeter and the information on the soil type, land cover form and management of the eight different agricultural ecosystems.

series were filled linearly, i.e., lysimeter (gap size: 2-minutes), soil surface temperature (T_{surf}: 6-hours), leaf wetness (LWS: 10-minutes) and visibility (10-minutes). A linear regression model with the same land cover type (grass, wheat) was used to fill the gaps for T_{canopy}.

2.4. Determination of non-rainfall water

We developed a refined identification system that uses a specific criterion to determine NRWI components, similar to the methods of Zhang et al. (2019a). The refined scheme tries to overcome shortcoming of previous methods (Groh et al., 2018; Zhang et al., 2019a; Paulus et al., 2024) by using i) air visibility to better define fog, ii) leaf wetness devices placed in the top layer of the canopy to define the time of dew formation, and iii) surface temperature to distinguish dew from frost and fog from rime. We did not use the surface temperature to estimate the dew point temperature because no RH measurements were available for the corresponding canopy surface layer. The schematics of the identification system are shown in Fig. 2 and are defined as follows.

- **Rain/snow:** The mass increase of the lysimeter monolith was separated into times with precipitation and without precipitation. We used the output of present weather codes from the visibility device on a 1-minute basis. This SYNOP codes (surface synoptic observations) are numerical codes used to report weather observations from weather stations. They include information on different forms of liquid, freezing and solid precipitation, with different intensity levels (slight, moderate or heavy), including drizzle, hail, showers and intermittent precipitation (SYNOP codes 40 to 45, 50 to 58, 60 to 68, 70 to 77, and 80 to 89). Standard rain gauges often underestimate precipitation or are unable to detect small rain events compared to precipitation from weighable lysimeters (Schnepper et al., 2023). Therefore, we also defined an increase in lysimeter weight as precipitation if we detected an increase in lysimeter weight within a 3-hour window before and after the rain and no dew/frost or fog/hoarfrost (definition see below) occurred during this time.

In a second step other events were separated into different NRWI.

- **Fog/Rime:** Fog/rime time was defined when the visibility was below 1 km, when SYNOP codes indicated fog (20, and 30 to 35) or mist (10). We attributed the increase in lysimeter weight to dew rather than to mist/fog when identifying time with both dew and fog during an event with mist, as the visibility device did not have a HygroVue sensor in order to differentiate between haze and mist. The fog time was extended by one hour before and after each event to allow for the possibility of fog or mist forming below 1.5 m where visibility is measured.
  - The mass increase was defined as **fog** when the plant or soil surface temperature (T_{canopy}) was above 0°C.
  - The mass increase was defined as **rime** when the plant or soil surface temperature (T_{canopy}) was $\leq$ 0°C (freezing point).
  - **Mix fog/rime** and **rain**: We defined fog/rain as a mixed fog/rime event with rain if rain was detected 3 h before and after the fog/rime event, and as fog/rime if the rain occurred more than 3 h before or after the fog/rime event.
- **Dew/frost**: we defined the time of dew or frost occurrence based on the information of the LWS and when air visibility range was larger than 1 km (excluding mist). The LWS sensor reacts differently to dew formation, frost and rain events and we used a code developed by Binks et al. (2021) to define time of dew and frost. We observed an earlier response of the lysimeter mass gain compared to the sensed LWS values, suggesting that dew or frost formation in the canopy often started much earlier than observed by the LWS. Due to difficulties in detecting dew/frost events in winter with long nighttime duration, persisting daytime frost, early onset of dew/frost formation, and a general problem of the code by Binks et al. (2021) to

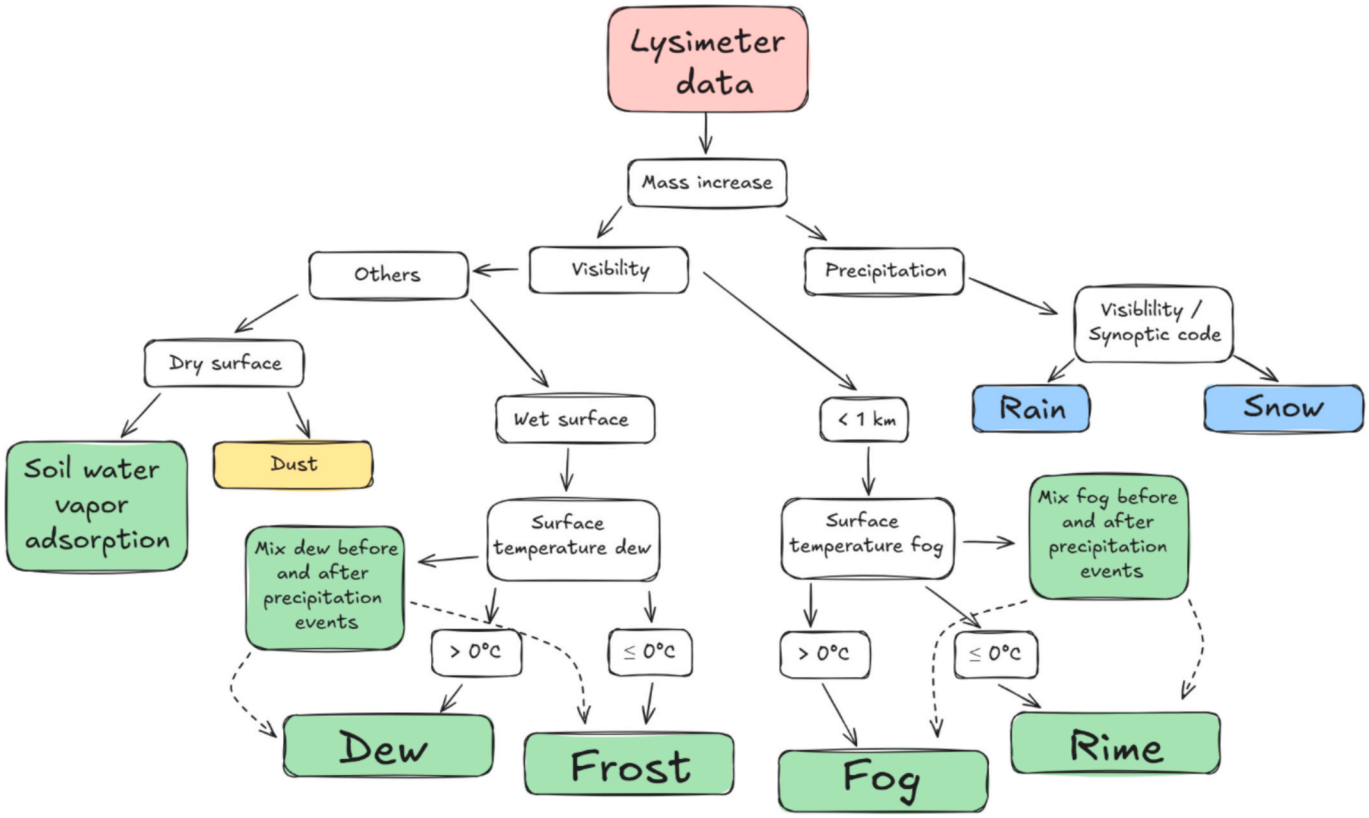

Fig. 2. Schemata for the identification system of the different non-rainfall water inputs, i.e., soil water vapor adsorption, dew, frost/ frozen dew, rime, and fog.

detect frost, we have extended the dew/frost period (10 h before and 5 h after the event) to allow a more accurate quantification of frost.
  - o **Dew**: Lysimeter mass increases were defined as dew when the plant or soil surface (T_{canopy}) was $> 0°C$ and the LWS sensor detected dew times (Groh et al., 2018).
  - o **Frost**: The same was done for frost, except that the plant or soil surface (T_{canopy}) was $\leq 0°C$ (Wisniewski, 1982).
  - o **Mix dew/ frost** and **rain/snow**: We define dew/frost as a mixed dew/frost event with rain if rain is expected 3 h before and after the dew/frost event, and as dew/frost if the rain occurred more than 3 h before or after the dew/frost event. This was necessary to exclude from the investigation any possible transition from a dew/ frost event before or after rainfall/snowfall.
- **WVA**: was defined for times of mass increase in the lysimeter weight and a dry surface of the LWS and a visibility > 1 km. In general, WVA occurs when the water vapor pressure in air-filled pores is lower than the vapor pressure in the atmosphere. In theory, direct adsorption may occur in cases of fog or dew formation if a downward gradient is maintained and the soil moisture is extremely dry, with moisture contents close to the wilting point. However, once dew forms or fog deposition begins on the surface, the soil moisture at the surface is relatively high (e.g., approaching saturation), such that a downward gradient of water vapor from the atmosphere, and thus WVA, is prevented. As it is unlikely to occur simultaneously at the macro-scale, we assume that a phase change of water from vapor to liquid in the soil is negligible, before dew formation and fog deposition start at the surface. In addition, weekly dust samples were taken with a dry deposition device to exclude the possibility of dust deposition biasing the determination of WVA.

Based on this experimental set-up and the mentioned schemata, all different NRWI of the corresponding soil type and vegetation under the same climatic conditions could be estimated. We compared our results with an established identification system for NRWI (Zhang et al., 2019a), which uses relative humidity of 100 % at 1 m height as a criterion for quantifying fog amounts during periods of increasing lysimeter mass. Any further increase of lysimeter mass in the absence of rainfall, dust or fog was classified as dew formation or WVA. Zhang et al. (2019a) defined dew formation as occurring when the soil surface temperature was below the dew point at 1 m above ground, and any other mass increases in the lysimeter were attributed to WVA. Please note we used for the estimation of the dew point meteorological observations from 2 m above ground. See supplementary material (Fig. S2, Fig. S3, Fig. S4) for an example time series of a dew and fog, dew and rain event between the two methods and the corresponding change in the lysimeter mass.

2.5. Data analysis

For the comparison of dew, frost, fog, rime and WVA between the different land cover types, the Wilcoxon rank sum test was used to determine whether the differences between them were significant. The Spearman rank correlation coefficient was used to characterize the monotonic relationship between soil and meteorological variables, i.e., T_{air}, W_s, RH, G_s, SWC, T_{soil}, T_{intC}, T_{canopy}, and R_n and the NRWI. A period, when water availability to plants was limited (May to June 2023), and to exclude confounding effects in time with large differences in plant surface cover, was chosen to identify the main environmental variables affecting NRWI in the eight different ecosystems. The coefficients were classified according to the following three classes i) weak (> -0.39 & < -0.1 or > 0.1 & < 0.39), ii) moderate (>-0.69 & < -0.4 or > 0.4 & < 0.69), and iii) strong (< -0.7 or > 0.7).

3. Results

3.1. Choice of the NRW identification method

The refined method resulted in an average dew/frost formation of 12.30 mm across all land cover types (Fig. 3) over the observation period (i.e., nine months), while the dew formation obtained by the method of Zhang et al. (2019a) estimated a much higher average value of 19.06 mm, which corresponds to an elevated over-estimation of dew by 55 %. This was also the case for WVA, where our refined method estimated 0.22 mm and the method of Zhang et al. (2019a) reached 5.57 mm (elevated estimation by: 2522 %). Meanwhile, for fog/rime, the method proposed by Zhang et al. (2019a) indicated no occurrence of fog at all, while our refined method based on a visibility device showed an average fog deposition of 3.40 mm over the nine months observation period. Thus, the NRWI identification system proposed by Zhang et al. (2019a), which lacked the visibility device, did not detect fog. Note that the time series between lysimeters may differ in length due to gaps in the measurement data for the comparison and thus do not interpret the absolute values from Fig. 3.

The distribution of dew/frost, fog/rime and WVA data also differed between methods (Fig. 3). The distribution of dew/frost data showed a narrow range with our refined method, which was not the case when data were estimated according to Zhang et al. (2019a). Also, distribution for dew/frost formation between the two land cover types with the refined method did not overlap, in contrast to the method of Zhang et al. (2019a) (Fig. 3, upper and right parts). For WVA, our refined assessment indicated a much smaller range for the arable land and grassland data than indicated according the method of Zhang et al. (2019a). For fog/ rime, there were little of any differences between land cover types, suggesting that canopy and surface characteristics of plants were less important for this type of NRWI.

The proportion of mixed dew/frost and rain/snow events to total dew/frost was on average 42 % and 79 % for the grassland and arable land (i.e., winter wheat) land cover types, respectively. The proportion

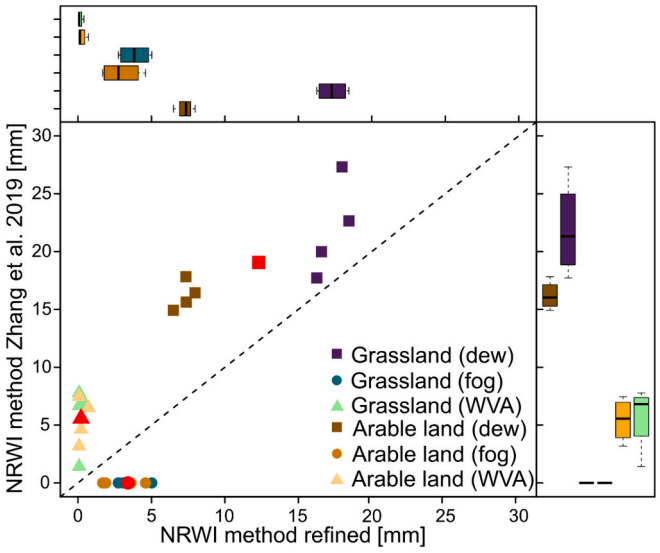

Fig. 3. Comparison of the methods for identifying non-rainfall water inputs (NRWI) for dew/frost, fog/rime and soil water vapour adsorption (WVA) between the method proposed by Zhang et al. (2019a) and the refined method presented here. The soil surface temperature was used in the method of Zhang et al. (2019a) to distinguish between the occurrence of dew and WVA. The red symbols show the average dew/frost, fog/rime and WVA across all ecosystems for both methods. The distribution of the corresponding data is shown beside and above with box plots for each method, NRWI fraction and land cover type. (For interpretation of the references to colour in this figure legend, the reader is referred to the web version of this article.)

of mixed fog/rime and rain/snow events to total fog/rime was on average 63 % and 92 % for the grassland and arable land land cover types respectively. This shows that a significant amount of NRWI at Selhausen entered the ecosystem just before or after rain/snow events.

3.2. Variability of NRWI across natural and agricultural ecosystems

The main share of NRWI comes from dew formation across all eight land covers (see Fig. 3). Average hourly dew formation, calculated for the time when all eight land covers provided data, showed that the average hourly dew formation rates for the four arable land cover types ranged from 0.042 to 0.059 mm/h, which was significantly greater (Wilcox test p-value 0.02) than those of the average dew formation rates for the grassland covers (range: 0.030 to 0.039 mm/h). However, based on the total number of hours in which dew formation occurred and measurements were available, dew occurred more frequently on grass than on winter wheat.

Frost formation reached much smaller rates at Selhausen compared with dew formation, and frost formation rates did not show any significant difference between the land cover types. Fog deposition rates, in turn, were slightly larger than for rime but did not show clear differences between land cover types, neither for fog nor for rime. The hours during which fog or rime occurred were also very similar in the two land cover types. However, fog occurred more frequently (43 h, on average) than rime (2 h, on average).

There were only two lysimeters that showed WVA when data were available for all the lysimeters, and the rates and the number of hours during which this WVA occurred were very low. Note that the sums shown for the different NRWI in Table 1 are smaller than those shown in Fig. 3, as only observations where all lysimeters provide observations are included in Table 1. The error margins were generally low for the respective NRWI fractions and did not differ in magnitude between soils, thus supporting the robustness of the differences between land cover forms.

The difference for the water fluxes at night between lysimeters with different land cover type is illustrated in Fig. 4. The three examples show a typical dew formation event (Fig. 4 A), different water flow directions (dew and evapotranspiration, Fig. 4 B) and a within canopy nocturnal water cycle (Fig. 4 C). The case with different flow directions (Fig. 4 B, C) explains why the grassland had a much greater frequency of dew formation during the observation period compared to the winter wheat. However, the latter example (C) shows that there was not only a difference in water flow direction between lysimeters with grass or winter wheat, but also in the presence of a nocturnal water cycle within canopy as the lysimeters showed in Fig. 4 C a clear weight loss due to evapotranspiration, and the leaf wetness sensor, installed at the canopy top, showed dew formation. These observations suggest that, for vegetation with a larger canopy, evaporation and dew formation may occur simultaneously at different heights within the canopy.

To gain a deeper insight into the frequency of these difference in flow directions between the land cover types grassland and arable land (winter wheat), we calculated the times of occurrence of dew on an hourly basis for each land cover type when all lysimeters provided data. We then averaged the time series of dew occurrence for the grassland and winter wheat lysimeters. The comparison showed that in 83.8 % of the comparable hours, dew formation occurred on grassland, whereas winter wheat showed evapotranspiration as shown exemplarily in Fig. 4 B. In 1.6 % of the hours, winter wheat showed dew formation, while grassland still lost water by evapotranspiration and in 14.6 % of the cases, both grassland and winter wheat showed dew formation.

3.3. Relationship between environmental variables and NRWI

To disentangle environment controls on dew formation, the dew events before and after rain events (mix of dew and rain) have not been considered here to avoid confounding the analysis. For the other data,

Table 1
Average rate. error margins (in brackets), hour of occurrence, and the amount of dew, frost, fog, rime and soil water vapor adsorption (WVA) for the times when all ecosystems provided data over the observation period from October 2022 to June 2023 at Selhausen.

Land cover type	Origin	Dew			Frost			Fog			Rime			WVA		
		mm/h	∑h	mm	mm/h	∑h	mm	mm/h	∑h	mm	mm/h	∑h	mm	mm/h	∑h	mm
Grassland	Nancy	0.030 (±0.00070)	184.8	6.12	0.013 (±0.00004)	40.2	0.50	0.041 (±0.00027)	41.6	1.67	0.031 (±0.00009)	1.9	0.1	0.002 (±0.000006)	0.73	0.00
	Scheyern	0.034 (±0.00074)	183.6	6.22	0.012 (±0.00003)	53.6	0.63	0.039 (±0.00031)	42.7	1.67	0.044 (±0.00012)	1.9	0.1	0.000	0.00	0.00
	Rollesbroich	0.039 (±0.00078)	175.4	6.84	0.015 (±0.00006)	56.8	0.85	0.037 (±0.00041)	39.6	1.47	0.030 (±0.00013)	2.7	0.1	0.000	0.00	0.00
	Wüstebach	0.036 (±0.00068)	163.5	5.83	0.012 (±0.00008)	67.6	0.83	0.038 (±0.00038)	43.1	1.64	0.026 (±0.00010)	3.1	0.1	0.000	0.00	0.00
Arable land (winter wheat)	Bad Lauchstädt	0.042 (±0.00073)	81.5	3.44	0.018 (±0.00005)	6.5	0.12	0.039 (±0.00041)	46.0	1.81	0.040 (±0.00011)	1.9	0.1	0.000	0.00	0.00
	Selhausen	0.051 (±0.00077)	76.5	3.88	0.018 (±0.00011)	5.7	0.10	0.032 (±0.00031)	46.2	1.47	0.042 (±0.00012)	1.9	0.1	0.001 (±0.000002)	0.18	0.00
	Dedelow	0.059 (±0.00082)	84.6	4.97	0.013 (±0.00005)	6.1	0.08	0.033 (±0.00028)	44.1	1.47	0.040 (±0.00013)	1.9	0.1	0.000	0.00	0.00
	Sauerbach	0.048 (±0.00073)	101.0	4.82	0.019 (±0.00008)	7.7	0.14	0.035 (±0.00030)	42.3	1.49	0.035 (±0.00008)	1.7	0.1	0.000	0.00	0.00

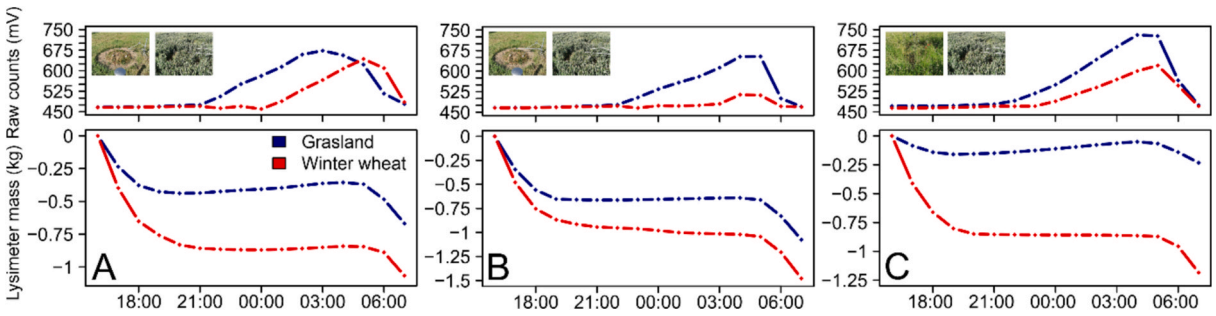

Fig. 4. Examples of diurnal water fluxes and leaf wetness for two lysimeters with different land cover type (grassland and arable land/winter wheat) for different situations: A) dew formation for both ecosystems with soils from Rollesbroich and Bad Lauchstädt (5 June 2023), B) different water flow directions with dew formation (Rollesbroich grassland) and evapotranspiration (Bad Lauchstädt winter wheat, 15 June 2023) and C) dew formation (Wüstebach grassland) and a case with an inner canopy water cycle for winter wheat, where dew formation is detected at the canopy top, but evapotranspiration is observed by the lysimeter (Bad Lauchstädt, 11 June 2023).

the relationship between different environmental variables and the dominant NRWI fraction i.e., dew on an hourly basis during the dry period, shows distinct differences between land surface covers with grass and winter wheat, respectively. For grassland cover, dew formation was weakly correlated with W_s (negative) and RH (positive), whereas soils covered with winter wheat did not show any significant correlation with both variables (Fig. 5 A, B). Soil heat flux (G_s) and dew formation were only weakly related, and the respective correlations

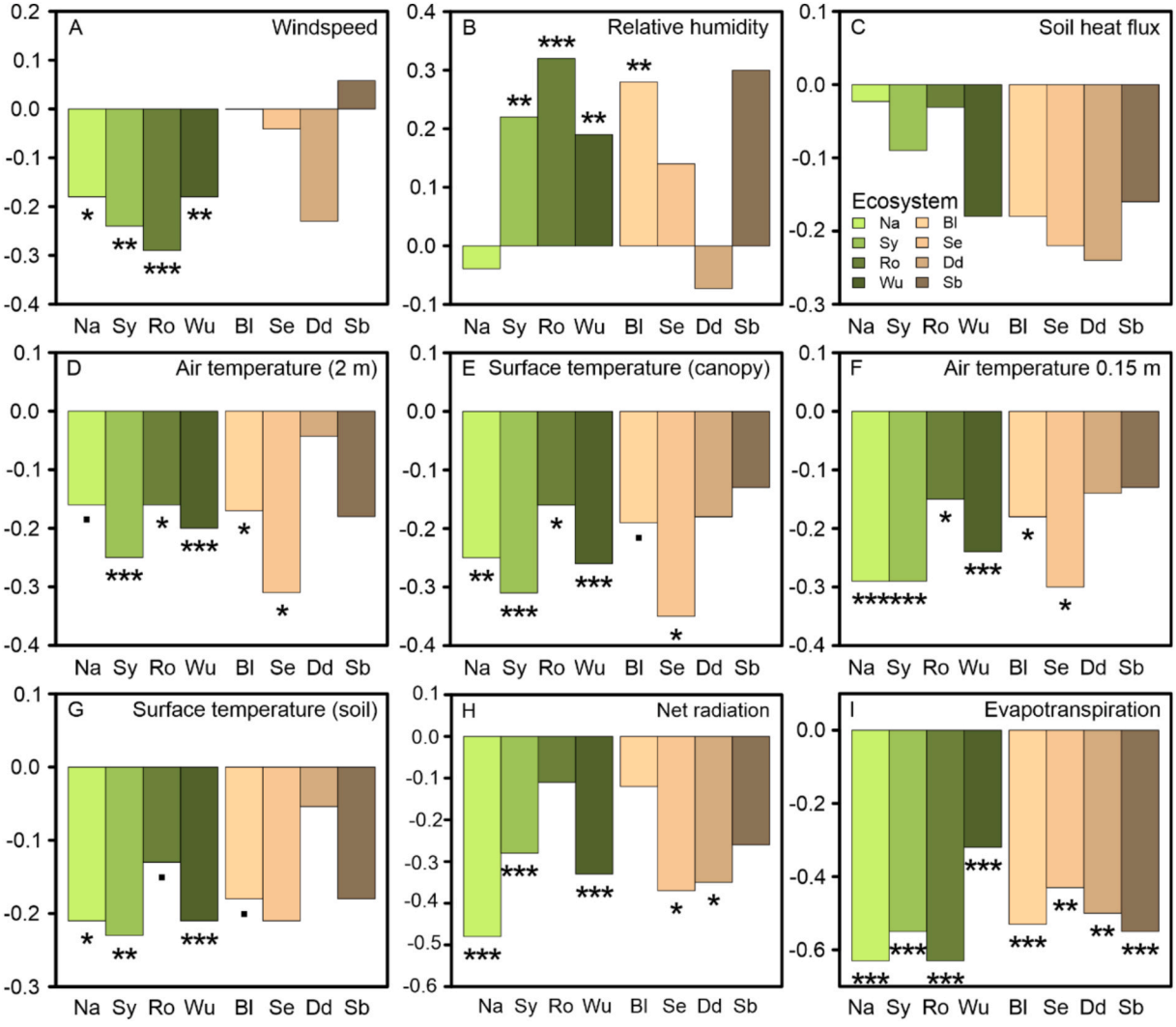

Fig. 5. Spearman correlation coefficient between dew and environmental drivers for the eight ecosystems from Nancy (Na), Scheyern (Sy), Rollesbroich (Ro), Wüstebach (Wu), Bad Lauchstädt (Bl), Selhausen (Se), Dedelow (Dd), and Sauerbach (Sb) at Selhausen. The different colours represent the different land cover types, i.e. grassland (green) and arable land (brown). The different significance levels are marked with the symbols "***", "**", "*" and "." for the p-values (0, 0.001, 0.01 and 0.05), respectively. (For interpretation of the references to colour in this figure legend, the reader is referred to the web version of this article.)

were not significant for ecosystems with a larger vegetation such as for winter wheat and soil from Wüstebach with large permanent grass cover. Dew formation for grassland and arable land was significantly but still weakly correlated with temperature related variables. Only the lysimeters from Dedelow and Sauerbach did not point to significant relationships, because only a few observation variables were available for the correlation analysis. However, the T_{canopy} showed overall the largest correlation coefficients with dew formation. R_n was in most cases weakly and significantly correlated with dew. Only the grassland from Nancy, which was a packed Technosol, showed a moderate respective correlation. Besides, all eight cover types showed a significant and moderate negative correlation between dew formation and evapotranspiration for hourly time steps. Yet, in no case, any single parameter explained more than 50 % of data variability (Fig. 5).

4. Discussion

4.1. Choice of the NRW identification method

In 2019, Zhang et al. (2019a) were among the first to identify NRWI partitioning. Yet, when developing their method, the authors did not have access to the highly equipped weighed lysimeters as used here, rendering it difficult to monitor each NRWI compartment. Here, the method to identify the different NRWI as proposed by Zhang et al. (2019a) led, in general, to larger values of estimated dew and WVA, and to smaller estimates of fog compared with the refined identification method proposed here. For fog, the RH never achieved values of 100 %, thus leading to a clear underestimation of fog by the method proposed by Zhang et al. (2019a). Similar findings were already mentioned by Paulus et al. (2022), who have set the value of RH reading to a value of 97.1 % at their site to account for systematic biases and drifts of the RH sensor. In general, foggy conditions might already start earlier than RH of 100 % (Klemm and Lin, 2016). This problem was addressed here by using an air visibility measuring device instead of a RH sensor, which helped to reduce the uncertainty in determining the NRWI component of fog (see example in Fig. S2). Such devices have been widely used in fog research in the past, especially in meteorology (e.g., Price, 2011; Herckes et al., 2015; Weedon et al., 2024), and seem, thus, needed to increase accuracy in NRWI assessment.

The larger estimates of dew formation with the identification system proposed by Zhang et al. (2019a) could be explained by the use of the estimated dew point temperature, which was to define when dew or WVA occurs. Yet, the dew point is estimated based on observations from T_{air} and RH sensors installed at 2 m above the ground, and formation of dew is assumed once the soil surface temperature was below the estimated dew point temperature. However, in most cases there are vertical gradients of RH and T_{air} above the soil and plant surfaces (Ney and Graf, 2018; Simó et al., 2018; Weedon et al., 2024). These gradients alter dew point temperatures at the respective height above ground where dew formation starts, and this alteration could not yet be accounted for in the method of Zhang et al. (2019a). Thus, often during dew events, dew formation is partially related to WVA instead of dew, as shown in Fig. S3.

Beside the lacking considerations of gradients, the use of the T_{surf} increases the bias when estimating NRWI by the method of Zhang et al. (2019a), since in smaller vegetation types (excluding forest), dew formation is more pronounced in the canopy layer than in the near-surface layer of a grassland or arable-land cover type (Jacobs et al., 1990; Wilson et al., 1999; Ritter et al., 2019; Xie et al., 2021). Therefore, we also tested the method using T_{canopy} rather than T_{surf}, which in their method is used as a criterion to decide whether dew or WVA occurs when the corresponding temperature is below the dew point temperature at reference height of the meteorological observation (here 2 m). When basing calculations on T_{canopy}, we obtained a smaller estimate of WVA, which reduced from an average of 5.57 mm to 1.97 mm. However, we also found that the average dew formation increased from 19.06 mm to 22.66 mm. Compared to our refined method, this corresponds to an increase from 55 % to 84 % (see Fig. S5).

Our data are in good agreement with findings of Kidron et al. (2023), who showed for several sites in a desert (Negev) that the meteorological conditions for dew formation at 1 m above the ground differed substantially from those measured at the soil or rock surface. Similarly, Lloyd (1961) showed for a grassland site in northern Idaho that dew formation from 0.3 m to a height of 1.5 m increased, on average, from 0.1 mm to 0.19 mm. However, we also found that the LWS sensors often responded with a delay compared to the increase in lysimeter weight during periods of dew formation (e.g., see Fig. 4 C), especially in winter. To better detect the beginning and end of dew events with our set-up, it is necessary to better understand in the future why the artificial surfaces of the LWS sensors indicate dew formation with a delay, e.g., because the artificial leaf cools down more slowly than the leaves of the vegetation, or because there were other material-related obstacles to dew formation on the artificial leaf of the LWS sensor. In addition, the minimum dew drop detectable by these sensors could lead to uncertainty in defining the exact start and end of dew formation (Beysens, 2018). Ideally, such artificial condensation surfaces should have comparable wetting properties, which are critical for nucleation and growth, as well as similar emissivity and low thermal mass as natural leaves, which are essential for dew formation and dew growth. This clearly demonstrates the importance of high precision lysimeters in determining NRWI such as dew formation. In general, the method could also be used in different climatic regions, such as arid (extremely dry) and tropical (very humid) areas. However, the delayed response of the LWS sensor at this site should be revisited, as this may be related not only to the intrinsic properties of the sensor, but also to the properties of the canopy and the installation height of the LWS sensor. This is crucial for determining dew/frost, as well as for distinguishing between dew/frost and WVA. It is conceivable that WVA occurs more frequently in semi-arid and arid regions than in more humid conditions. Therefore, for such ecosystems, the lag time should be revised to reduce possible bias when distinguishing between the two NRWI components.

Another difference between the identification methods is that the Zhang et al. (2019b) method has a class called 'Others', which at 4.6 % is similar in magnitude to the contribution of dew (5 %) and WVA (5.1 %) in their study. This ‘Others’ class quantifies the inaccuracy in the determination of NRWI and/or precipitation, which did not occur with the refined method. Possible reasons for this are that precipitation sensors, especially of the tipping bucket type, often underestimate precipitation (Hoffmann et al., 2016; Schnepper et al., 2023; Tall et al., 2023) under conditions with very light precipitation or drizzle, that they react with a delay, issues due to heating, or that the criteria for classification of fog, dew and WVA are not met by the sensors. Here we included such transition times via a class that describes water as a mix of NRWI and rain/snow or for rain/snow. This was necessary because the increase in lysimeter weight due to rain/snow was sometimes detected by the averaging routine of the AWAT filter at an earlier start of the weight increase, depending on rain intensity, rain duration and total precipitation amount. Nevertheless, moist air conditions before, during and after a rain event may also create conditions conducive to fog deposition. For example, advective fog occurs when moist air moves horizontally above a cold surface. Tardif and Rasmussen (2008) reported that liquid precipitation increases the likelihood of fog formation. Also, increased moisture in the air enhances the probability of dew formation as it contains more water vapor, and when the air close to saturation, a small decrease in temperature might be enough to start the condensation process. In such circumstances, it is difficult to clearly distinguish between rain and NRWI. The use of high-frequency stable isotopes of hydrogen and oxygen could be here helpful, as they provide information about the formation process (Rothfuss et al., 2013; Kaseke et al., 2017; Tian et al., 2019; Tian et al., 2021; Tian et al., 2022). This could help improve the separation between dew, fog, and rainfall.

The surface and canopy properties differ between grassland and arable-land covers, which was captured well by our refined method. The

method by Zhang et al. (2019a) showed a smaller difference, compared to us, in dew formation between winter wheat, but a larger difference between the different grasslands. The clear discrepancies of dew distribution between the different land covers clearly indicates that microclimatic conditions near the soil and plant surface are different from those observed at 2 m above the ground. In addition, using T_{canopy} instead of T_{surf}, significantly changed the occurrence of dew in the arable land and grassland, demonstrating the uncertainty in determining NRWI according to Zhang et al. (2019a). Although T_{canopy} has improved the detection of dew formation, still lysimeter mass increases often gets classified as dew before, during, and after rainfall events (e.g., see Fig. S4). Lembrechts (2023) recently pointed out that microclimate is more important than macroclimate when it comes to the migration and survival of terrestrial organisms in their habitats, especially under the current rapidly changing conditions due to climate change. Improving the identification and prediction of dew and other NRWI components is thus also important for other disciplines aside hydrology. This is particularly evident here for water inputs to different land surface covers.

The uncertainty in defining the onset and end of dew formation using the method of Zhang et al. (2019a) also affected the quantification of WVA, resulting in larger estimates of WVA. Zhang et al.'s method often misclassifies dew formation as WVA because the soil surface temperature is not below the dew point temperature at a height of 2 m (Fig. S3). Yet, the lesser occurrence of WVA as determined here with our refined methodology was consistent with other recent investigations at the study site (Paulus et al., 2024). Paulus et al. (2024) pointed out that, even when considering the extreme dry year of 2018, WVA does not play a prominent role at the site under such temperate climatic conditions. This is consistent with our findings. Several other studies have shown that WVA contributes more water to the ecosystem than was observed in this study (e.g., Agam and Berliner, 2006; Verhoef et al., 2006; Saaltink et al., 2020; Paulus et al., 2025). However, given that the contribution of WVA to the NRWI is low compared to dew/frost or fog/rime under a temperate climate, it is not surprising, as soil needs to be relatively dry and considering that the relative humidity of the air in the soil is still almost 100 % even at the permanent wilting point. In temperate regions, there is usually sufficient moisture in the system for the soil water content to rarely drop below the wilting point. Therefore, WVA is unlikely to occur under these conditions. Testing this approach in locations with arid or semi-arid conditions in the future would help verify whether the WVA can be accurately determined using the existing rules or if further conditions are required to do so under such conditions.

4.2. *Variability of NRWI across natural and agricultural land covers*

Average dew rates during the observation period differed significantly between vegetation types, grassland and winter wheat. Previous studies have shown that both meteorological conditions and surface characteristics influence dew formation, such as soil texture, cobblestones, pebbles, and vegetation (Li, 2002; Xiao et al., 2009; Kidron et al., 2024a). In our case we can exclude that meteorological conditions drove differences in dew formation, since all eight land covers at the Selhausen site had been exposed to the same macroclimate. The ecosystems differed in land cover and soil types only.

The lesser dew formation observed in the winter wheat ecosystems might be attributed to two factors: the different density of vegetation cover and the physiological characteristics of the plants. The lysimeter covered with winter wheat was sparsely vegetated after sowing in late October (2022–10-24) relative to the grassland plots. In the arable ecosystem, therefore, soils prevailed sparsely vegetated from October until a new fully developed stand had developed in April/June 2023. Hence, the vegetation surface of the lysimeter with arable soil had a significant smaller surface area than the lysimeter under grassland, in the period from autumn to spring. As sparsely vegetated or bare soils do not cool down as quickly as leaves during the night, there is less radiative heat loss (Xiao et al., 2009), and, hence, also less dew formation. On the other hand, during the growing season increased plant density (e.g., canopy structure and leaf area index) also affects leaf temperature reduction (Winkel et al., 2009), which is critical for dew formation during clear and calm nights. The differences can be large, as seen in Fig. 6, which shows the diurnal canopy temperature for the grassland and winter wheat lysimeter. This demonstrates that canopy temperature can vary significantly depending on land cover type, both during the day and at night. Hence, and beside the macroclimatic conditions, also the type of land surface cover (i.e. density, structure, diversity) and soil properties (e.g., longwave emissivity, thermal conductivity) play a crucial role in dew formation processes. Also, Ran et al. (2024) showed that ecosystems covered with *Artemisia ordosica* in a semi-arid region (China) experienced greater dew formation compared to bare soil conditions, and Xiao et al. (2009) showed that the type of vegetation (i.e. grass vs. crop) had a strong influence on the occurrence of dew in central Europe (Falkenberg, Germany). The authors outlined that dew was always detectable earlier over grassland than over winter wheat (Fig. 4). This may be due to leaf characteristics, as the wider leaves of wheat may create a 'decoupled' atmosphere within the canopy that takes longer to cool and condense overnight. In contrast, the thin, vertical grass leaves encounter the cold air more quickly than the winter wheat. Once condensation begins over the winter wheat, its larger surface area may account for the greater amount of dew. The results of these studies are consistent with ours, that grass ecosystems generally increase the incidence of dew, but once crop vegetation develops, dew rates can be much larger than in grassland under the same macroclimate.

Plant-specific properties also contribute to the spatial differences in water fluxes at night at the study site: the winter wheat cover often lost water by evapotranspiration at night, whereas the grassland gained water by dew formation. The nocturnal water losses, occurred more frequently under winter wheat, suggesting that the respective stomata of the plants were not completely closed at night. Hence, water could still escape through the cuticle, while blockages in the guard cells likely

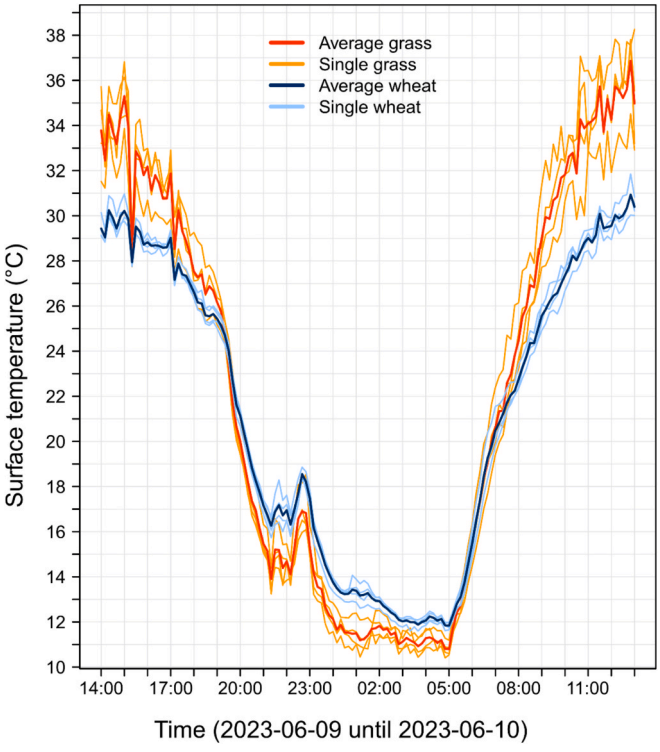

Fig. 6. Diurnal surface temperatures for an exemplary night in June 2023, for the individual lysimeter and for average grassland and winter wheat.

prevented the stomata from closing (Resco de Dios et al., 2019). Several other studies confirmed that different types of land use and plants do lose significant amounts of water at night. (Groh et al., 2019; Han et al., 2020; Padrón et al., 2020). According to Schoppach et al. (2014), the nighttime transpiration is mainly sensitive to air temperature and vapor pressure deficit. Lu et al. (2023) showed that the respective water loss occurred mainly through the stomata to support respiration.

The difference between surface water fluxes at larger scale at night might also have implications for atmospheric dynamics, as condensation releases heat and therefore unequal dew distribution creates also increased patchiness in the near surface temperature. Small-scale surface variability (tens of metres) will probably not have an impact, but for large adjacent fields (with a scale of 100 m or more), some with dew and some without, this fact contributes to the thermal contrast between fields, which can lead to local lateral advection and even turbulent mixing (Cuxart et al., 2016).

In summary, the complexity of the nocturnal water fluxes showed that divergent processes occurred within the stand. If evapotranspiration and dew formation (canopy) occur simultaneously (Fig. 4 C), we assume that the source of condensed water within the stand boundary to the atmosphere comes to a large extend from the soil (upward flux) and not only from the atmosphere (downward flux) as in classical dew formation. Monteith (1957) referred to this process as soil distillation: when the water source comes from the soil, it should occur mainly at clear nights and in light winds. In our case, the meteorological conditions were sufficient to cause condensation on the foliage near the canopy top, but also to remove some of the water vapor transported from the soil from the stand (evaporation). Using stable isotope techniques, Li et al. (2021) reported for an alpine grassland that distillation contributed by 9 % to 42 % to the total NRWI. Thus, the inclusion of water-stable isotopes in addition to our present setup could help to even better understand water origin and flux processes within the canopy at night.

4.3. Relationship between environmental variables and dew

When exploring the relationship between different environmental variables and the site dominant NRWI, dew formation during a dry period showed a significant negative correlation with W_s, which is consistent with previous results (e.g., Guo et al., 2016; Xu et al., 2023). The relationship with W_s was non-linear and favoured dew formation within a limited range of wind speeds. Light winds enhance dew formation by bringing additional moist air to the surface (Baier, 1966; Beysens et al., 2005; Guo et al., 2016). However, if the wind speed is too large, it inhibits dew formation (Beysens et al., 2005) and increases evaporation (Groh et al., 2019).

Both dew formation from grassland and arable-land ecosystems showed significant and negative correlations with different temperature related variables (T_{air}, T_{canopy}, T_{intC}, and T_{surf}) as well as with net radiation (R_n), as the latter promotes a further decrease in surface temperature by radiative cooling. Our results also showed that dew formation was weakly and positively correlated with RH for most land covers, which is consistent with previous studies (Pan et al., 2010; Zhuang and Zhao, 2014; Guo et al., 2016; Xu et al., 2023), as RH increases as temperature decreases, further increasing dew formation. The moderate correlation between evapotranspiration and dew formation on an hourly basis demonstrates that a rewetted surface might re-evaporate previously formed dew from the intercept of the plant and the soil.

5. Conclusions

In this investigation we quantified non-rainfall water inputs (NRWI) and assessed how they are influenced by different land cover types. This required the development of a refined identification system to distinguish between the different NRWI, i.e. dew, fog, and soil water vapor adsorption, all of which were quantified using high precision weighing lysimeters that were additionally equipped with an air visibility measuring device and leaf wetness sensors. This refined identification system for dew, fog, and soil water vapor adsorption revealed significant discrepancies to the original method of NRWI assessment by Zhang et al. (2019a), which overestimated mean average dew and soil water vapor adsorption amounts by 6.8 mm (55 %) and 5.4 mm (2552 %) respectively over the nine-month observation period. NRWI by fog was on average 3.4 mm and could only be detected with the refined method and not with the previous one.

We also found a significant difference between dew formation above the grassland and winter wheat surfaces, thus highlighting the importance of land cover types and their surface characteristics on dew characteristics which were not well resolved with the previous method. Dew was the main contributor to the total NRWI. It dominated in the grassland due to higher frequencies of dew formation. Compared to dew formation, the water input from fog was relatively small and the soil water vapor adsorption was negligible, as typical for this temperate climate. Arable crops lost more water at night through the process of transpiration (no closed stomata) or soil evaporation. The land cover type and their characteristics of vegetation play a decisive role in the formation of dew, as they influence the microclimate, which is essential for dew to form and grow.

CRediT authorship contribution statement

Jannis Groh: Writing – review & editing, Writing – original draft, Visualization, Software, Resources, Project administration, Methodology, Investigation, Funding acquisition, Formal analysis, Data curation, Conceptualization. **Thomas Pütz:** Writing – review & editing, Funding acquisition, Conceptualization. **Daniel Beysens:** Writing – review & editing. **Joan Cuxart:** Writing – review & editing. **Nurit Agam:** Writing – review & editing. **Werner Küpper:** Writing – review & editing, Data curation. **Paul D. Colaizzi:** Writing – review & editing. **Harry Vereecken:** Writing – review & editing. **Horst H. Gerke:** Writing – review & editing. **Wulf Amelung:** Writing – review & editing.

Declaration of competing interest

The authors declare that they have no known competing financial interests or personal relationships that could have appeared to influence the work reported in this paper.

Acknowledgements

We acknowledge the support of TERENO and SOILCan, which were funded by the Helmholtz Association (HGF) and the Federal Ministry of Education and Research (BMBF, Germany). We thank Werner Küpper, Andrea Ecker, Antonio Voss, Stephanie Stork, Ferdinand Engels, Philipp Meulendick, and Daniel Dolfus for their kind support at the lysimeter station in Selhausen. Part of the field experiments were supported by the Deutsche Hydrologische Gesellschaft e.V. (‘Feldstipendium’). Jannis Groh has been funded by the Deutsche Forschungsgemeinschaft (DFG, German Research Foundation, project no. 460817082). Also, Wulf Amelung acknowledges support from the Deutsche Forschungsgemeinschaft (DFG, German Research Foundation) under Germany's Excellence Strategy - EXC 2070 - 390732324.

Appendix A. Supplementary data

Supplementary data to this article can be found online at https://doi.org/10.1016/j.jhydrol.2026.135040.

Data availability

All quality proved data are available from the TERENO data discovery portal (https://ddp.tereno.net/ddp/). The data are searchable

via their site identification codes (lysimeter: se_y_011, se_y_013, se_y_021, se_y_023, se_y_031, se_y_033, se_y_041, se_y_043) and the meteorological (se_bdk_002) data.

References

Agam, N., Berliner, P.R., 2004. Diurnal Water Content changes in the Bare Soil of a Coastal Desert. J. Hydrometeorol. 5 (5), 922–933. https://doi.org/10.1175/1525-7541(2004)005<0922:Dwccit>2.0.Co;2.

Agam, N., Berliner, P.R., 2006. Dew formation and water vapor adsorption in semi-arid environments - a review. J. Arid Environ. 65 (4), 572–590. https://doi.org/10.1016/j.jaridenv.2005.09.004.

Aguirre-Gutiérrez, C.A., Holwerda, F., Goldsmith, G.R., Delgado, J., Yepez, E., Carbajal, N., Escoto-Rodríguez, M., Arredondo, J.T., 2019. The importance of dew in the water balance of a continental semiarid grassland. J. Arid Environ. https://doi.org/10.1016/j.jaridenv.2019.05.003.

Allen, R.G., Pruitt, W.O., Wright, J.L., Howell, T.A., Ventura, F., Snyder, R., Itenfisu, D., Steduto, P., Berengena, J., Yrisarry, J.B., Smith, M., Pereira, L.S., Raes, D., Perrier, A., Alves, I., Walter, I., Elliott, R., 2006. A recommendation on standardized surface resistance for hourly calculation of reference ETo by the FAO56 Penman-Monteith method. Agric Water Manag 81 (1–2), 1–22. https://doi.org/10.1016/j.agwat.2005.03.007.

Baier, W., 1966. Studies on dew formation under semi-arid conditions. Agric. Meteorol. 3 (1), 103–112. https://doi.org/10.1016/0002-1571(66)90008-2.

Ben-Asher, J., Alpert, P., Ben-Zvi, A., 2010. Dew is a major factor affecting vegetation water use efficiency rather than a source of water in the eastern Mediterranean area. Water Resour. Res. 46 (10). https://doi.org/10.1029/2008WR007484.

Beysens, D., Muselli, M., Nikolayev, V., Narhe, R., Milimouk, I., 2005. Measurement and modelling of dew in island, coastal and alpine areas. Atmos. Res. 73 (1), 1–22. https://doi.org/10.1016/j.atmosres.2004.05.003.

Beysens, D., 2018. Dew water. River Publishers series in chemical, environmental, and energy engineering. River Publishers, Gistrup.

Binks, O., Carle, H., Coughlin, I., da Costa, A.L., Meir, P., 2021. Measuring the vertical profile of leaf wetness in a forest canopy. MethodsX 8, 101332. https://doi.org/10.1016/j.mex.2021.101332.

Bogena, H.R., Montzka, C., Huisman, J.A., Graf, A., Schmidt, M., Stockinger, M., von Hebel, C., Hendricks-Franssen, H.J., van der Kruk, J., Tappe, W., Lücke, A., Baatz, R., Bol, R., Groh, J., Pütz, T., Jakobi, J., Kunkel, R., Sorg, J., Vereecken, H., 2018. The TERENO-Rur Hydrological Observatory: a Multiscale Multi-Compartment Research Platform for the Advancement of Hydrological Science. Vadose Zone J. 17 (1), 1–22. https://doi.org/10.2136/vzj2018.03.0055.

Chung, M., Dufour, A., Pluche, R., Thompson, S., 2017. How much does dry-season fog matter? Quantifying fog contributions to water balance in a coastal California watershed. Hydrol. Process. 31 (22), 3948–3961. https://doi.org/10.1002/hyp.11312.

Cuxart, J., Wrenger, B., Martínez-Villagrasa, D., Reuder, J., Jonassen, M.O., Jiménez, M. A., Lothon, M., Lohou, F., Hartogensis, O., Dünnermann, J., Conangla, L., Garai, A., 2016. Estimation of the advection effects induced by surface heterogeneities in the surface energy budget. Atmos. Chem. Phys. 16 (14), 9489–9504. https://doi.org/10.5194/acp-16-9489-2016.

Dawson, T.E., Goldsmith, G.R., 2018. The value of wet leaves. New Phytol. 219 (4), 1156–1169. https://doi.org/10.1111/nph.15307.

Degefie, D.T., El-Madany, T.S., Held, M., Hejkal, J., Hammer, E., Dupont, J.C., Haeffelin, M., Fleischer, E., Klemm, O., 2015. Fog chemical composition and its feedback to fog water fluxes, water vapor fluxes, and microphysical evolution of two events near Paris. Atmos. Res. 164–165, 328–338. https://doi.org/10.1016/j.atmosres.2015.05.002.

Evans, S., Todd-Brown, K.E.O., Jacobson, K., Jacobson, P., 2019. Non-rainfall Moisture: a Key driver of Microbial Respiration from standing Litter in Arid, Semiarid, and Mesic Grasslands. Ecosystems. https://doi.org/10.1007/s10021-019-00461-y.

Evenari, M., Shanan, L., Tadmor, N., 1982. The Negev. The Challenge of a Desert. The Negev, Second Edition. Harvard University Press, Cambridge, MA and London, England.

Fischer, D.T., Still, C.J., Williams, A.P., 2009. Significance of summer fog and overcast for drought stress and ecological functioning of coastal California endemic plant species. J. Biogeogr. 36 (4), 783–799. https://doi.org/10.1111/j.1365-2699.2008.02025.x.

Florentin, A., Agam, N., 2017. Estimating non-rainfall-water-inputs-derived latent heat flux with turbulence-based methods. Agric. For. Meteorol. 247, 533–540. https://doi.org/10.1016/j.agrformet.2017.08.035.

Goetz, J.D., Price, J.S., 2016. Ecohydrological controls on water distribution and productivity of moss communities in western boreal peatlands. Canada. Ecohydrology 9 (1), 138–152. https://doi.org/10.1002/eco.1620.

Goldsmith, G.R., Matzke, N.J., Dawson, T.E., 2013. The incidence and implications of clouds for cloud forest plant water relations. Ecol. Lett. 16 (3), 307–314. https://doi.org/10.1111/ele.12039.

Gottlieb, T.R., Eckardt, F.D., Venter, Z.S., Cramer, M.D., 2019. The contribution of fog to water and nutrient supply to Arthraerua leubnitziae in the central Namib Desert, Namibia. J. Arid Environ. 161, 35–46. https://doi.org/10.1016/j.jaridenv.2018.11.002.

Groh, J., Vanderborght, J., Pütz, T., Vereecken, H., 2016. How to Control the Lysimeter Bottom Boundary to Investigate the effect of climate Change on Soil Processes? Vadose Zone J. 15 (7), 1–25. https://doi.org/10.2136/vzj2015.08.0113.

Groh, J., Slawitsch, V., Herndl, M., Graf, A., Vereecken, H., Pütz, T., 2018. Determining dew and hoar frost formation for a low mountain range and alpine grassland site by weighable lysimeter. J. Hydrol. 563, 372–381. https://doi.org/10.1016/j.jhydrol.2018.06.009.

Groh, J., Pütz, T., Gerke, H.H., Vanderborght, J., Vereecken, H., 2019. Quantification and Prediction of Nighttime Evapotranspiration for two Distinct Grassland Ecosystems. Water Resour. Res. 55 (4), 2961–2975. https://doi.org/10.1029/2018wr024072.

Gultepe, I., Tardif, R., Michaelides, S.C., Cermak, J., Bott, A., Bendix, J., Müller, M.D., Pagowski, M., Hansen, B., Ellrod, G., Jacobs, W., Toth, G., Cober, S.G., 2007. Fog Research: a Review of Past Achievements and Future Perspectives. Pure Appl. Geophys. 164 (6), 1121–1159. https://doi.org/10.1007/s00024-007-0211-x.

Guo, X., Zha, T., Jia, X., Wu, B., Feng, W., Xie, J., Gong, J., Zhang, Y., Peltola, H., 2016. Dynamics of Dew in a Cold Desert-Shrub Ecosystem and its Abiotic Controls. Atmos. 7 (3), 32.

Han, Q., Liu, Q., Wang, T., Wang, L., Di, C., Chen, X., Smettem, K., Singh, S.K., 2020. Diagnosis of environmental controls on daily actual evapotranspiration across a global flux tower network: the roles of water and energy. Environ. Res. Lett. 15 (12), 124070. https://doi.org/10.1088/1748-9326/abcc8c.

Hanisch, S., Lohrey, C., Buerkert, A., 2015. Dewfall and its ecological significance in semi-arid coastal south-western Madagascar. J. Arid Environ. 121, 24–31. https://doi.org/10.1016/j.jaridenv.2015.05.007.

Herckes, P., Marcotte, A.R., Wang, Y., Collett, J.L., 2015. Fog composition in the Central Valley of California over three decades. Atmos. Res. 151, 20–30. https://doi.org/10.1016/j.atmosres.2014.01.025.

Hiatt, C., Fernandez, D., Potter, C., 2012. Measurements of fog Water Deposition on the California Central Coast. Atmospheric and Climate Sciences 02No.04, 7. https://doi.org/10.4236/acs.2012.24047.

Hoffmann, M., Schwartengräber, R., Wessolek, G., Peters, A., 2016. Comparison of simple rain gauge measurements with precision lysimeter data. Atmos. Res. 174–175, 120–123. https://doi.org/10.1016/j.atmosres.2016.01.016.

Jacobs, A.F.G., van Pul, W.A.J., van Dijken, A., 1990. Similarity moisture dew profiles within a corn canopy. J. Appl. Meteorol. 29 (12), 1300–1306. https://doi.org/10.1175/1520-0450(1990)029<1300:SMDPWA>2.0.CO;2.

Kaseke, K.F., Mills, A.J., Brown, R., Esler, K.J., Henschel, J.R., Seely, M.K., 2012. A Method for Direct Assessment of the "Non Rainfall" Atmospheric Water Cycle: Input and Evaporation from the Soil. Pure Appl. Geophys. 169 (5), 847–857. https://doi.org/10.1007/s00024-011-0328-9.

Kaseke, K.F., Wang, L., Seely, M.K., 2017. Nonrainfall water origins and formation mechanisms. Sci. Adv. 3 (3). https://doi.org/10.1126/sciadv.1603131.

Kidron, G.J., Kronenfeld, R., Starinsky, A., Xiao, B., Muselli, M., Beysens, D., 2023. Even in a dew desert: Dewfall does not provide sufficient moisture for biocrust growth – evidence from direct measurements and a meteorological model. J. Hydrol. 627, 130450. https://doi.org/10.1016/j.jhydrol.2023.130450.

Kidron, G.J., Kronenfeld, R., Xiao, B., Starinsky, A., McKay, C.P., Or, D., 2024a. Vapor flux induced by temperature gradient is responsible for providing liquid water to hypoliths. Sci. Rep. 14 (1), 23140. https://doi.org/10.1038/s41598-024-73555-w.

Kidron, G.J., Kronenfeld, R., Starinsky, A., 2024b. Mornings with the highest non-rainfall water during 2 years of measurements in the Negev–Ecological implications. Hydrol. Process. 38 (5), e15155. https://doi.org/10.1002/hyp.15155.

Klemm, O., Lin, N.H., 2016. What Causes Observed fog Trends: Air Quality or climate Change? Aerosol Air Qual. Res. 16 (5), 1131–1142. https://doi.org/10.4209/aaqr.2015.05.0353.

Knapp, A.K., Ciais, P., Smith, M.D., 2017. Reconciling inconsistencies in precipitation–productivity relationships: implications for climate change. New Phytol. 214 (1), 41–47. https://doi.org/10.1111/nph.14381.

Kohfahl, C., Molano-Leno, L., Martínez, G., Vanderlinden, K., Guardiola-Albert, C., Moreno, L., 2019. Determining groundwater recharge and vapor flow in dune sediments using a weighable precision meteo lysimeter. Sci. Total Environ. 656, 550–557. https://doi.org/10.1016/j.scitotenv.2018.11.415.

Kosmas, C., Danalatos, N.G., Poesen, J., van Wesemael, B., 1998. The effect of water vapour adsorption on soil moisture content under Mediterranean climatic conditions. Agric Water Manag 36 (2), 157–168. https://doi.org/10.1016/S0378-3774(97)00050-4.

Lembrechts, J.J., 2023. Microclimate alters the picture. Nat. Clim. Chang. 13 (5), 423–424. https://doi.org/10.1038/s41558-023-01632-5.

Li, B., Wang, L., Kaseke, K.F., Vogt, R., Li, L., K. Seely, M., 2018. The impact of fog on soil moisture dynamics in the Namib Desert. Advances in Water Resources, 113: 23-29, 10.1016/j.advwatres.2018.01.004.

Li, X.-Y., 2002. Effects of gravel and sand mulches on dew deposition in the semiarid region of China. J. Hydrol. 260 (1), 151–160. https://doi.org/10.1016/S0022-1694(01)00605-9.

Li, Y., Aemisegger, F., Riedl, A., Buchmann, N., Eugster, W., 2021. The role of dew and radiation fog inputs in the local water cycling of a temperate grassland during dry spells in central Europe. Hydrol. Earth Syst. Sci. 25 (5), 2617–2648. https://doi.org/10.5194/hess-25-2617-2021.

Liu, Z., Ballantyne, A.P., Poulter, B., Anderegg, W.R.L., Li, W., Bastos, A., Ciais, P., 2018. Precipitation thresholds regulate net carbon exchange at the continental scale. Nat. Commun. 9 (1), 3596. https://doi.org/10.1038/s41467-018-05948-1.

Lloyd, M.G., 1961. The Contribution of Dew to the Summer Water Budget of Northern Idaho. Bull. Am. Meteorol. Soc. 42 (8), 572–581. https://doi.org/10.1175/1520-0477-42.8.572.

Lu, Y., Jeffers, R., Raju, A., Kenny, T., Ratchanniyasamu, E., Fricke, W., 2023. Does night-time transpiration provide any benefit to wheat (Triticum aestivum L.) plants which are exposed to salt stress? Physiol. Plant. 175 (1), e13839. https://doi.org/10.1111/ppl.13839.

Malik, F.T., Clement, R.M., Gethin, D.T., Beysens, D., Cohen, R.E., Krawszik, W., Parker, A.R., 2015. Dew harvesting efficiency of four species of cacti. Bioinspir. Biomim. 10 (3), 036005. https://doi.org/10.1088/1748-3190/10/3/036005.
Marek, W.G., Evett, R.S., Gowda, H.P., Howell, A.T., Copeland, S.K., Baumhardt, R.L., 2014. Post-Processing Techniques for reducing Errors in weighing Lysimeter Evapotranspiration (ET) Datasets. Trans. ASABE 57 (2), 499. https://doi.org/10.13031/trans.57.10433.
Martins, C.S.C., Nazaries, L., Delgado-Baquerizo, M., Macdonald, C.A., Anderson, I.C., Singh, B.K., 2021. Rainfall frequency and soil water availability regulate soil methane and nitrous oxide fluxes from a native forest exposed to elevated carbon dioxide. Funct. Ecol. 35 (8), 1833–1847. https://doi.org/10.1111/1365-2435.13853.
McHugh, T.A., Morrissey, E.M., Reed, S.C., Hungate, B.A., Schwartz, E., 2015. Water from air: an overlooked source of moisture in arid and semiarid regions. Sci. Rep. 5, 13767. https://doi.org/10.1038/srep13767.
Meissner, R., Seeger, J., Rupp, H., Seyfarth, M., Borg, H., 2007. Measurement of dew, fog, and rime with a high-precision gravitation lysimeter. J. Plant Nutr. Soil Sci. 170 (3), 335–344. https://doi.org/10.1002/jpln.200625002.
Monteith, J.L., 1957. Dew. Quarterly Journal of the Royal Meteorological Society, 83 (357): 322-341, https://doi.org/10.1002/qj.49708335706.
Ney, P., Graf, A., 2018. High-Resolution Vertical Profile Measurements for Carbon Dioxide and Water Vapour Concentrations within and above Crop Canopies. Bound.-Lay. Meteorol. 166 (3), 449–473. https://doi.org/10.1007/s10546-017-0316-4.
Padrón, R.S., Gudmundsson, L., Michel, D., Seneviratne, S.I., 2020. Terrestrial water loss at night: global relevance from observations and climate models. Hydrol. Earth Syst. Sci. 24 (2), 793–807. https://doi.org/10.5194/hess-24-793-2020.
Pan, Y.-X., Wang, X.-P., Zhang, Y.-F., 2010. Dew formation characteristics in a revegetation-stabilized desert ecosystem in Shapotou area, Northern China. J. Hydrol. 387 (3), 265–272. https://doi.org/10.1016/j.jhydrol.2010.04.016.
Paulus, S.J., El-Madany, T.S., Orth, R., Hildebrandt, A., Wutzler, T., Carrara, A., Moreno, G., Perez-Priego, O., Kolle, O., Reichstein, M., Migliavacca, M., 2022. Resolving seasonal and diel dynamics of non-rainfall water inputs in a Mediterranean ecosystem using lysimeters. Hydrol. Earth Syst. Sci. 26 (23), 6263–6287. https://doi.org/10.5194/hess-26-6263-2022.
Paulus, S.J., Orth, R., Lee, S.C., Hildebrandt, A., Jung, M., Nelson, J.A., El-Madany, T.S., Carrara, A., Moreno, G., Mauder, M., Groh, J., Graf, A., Reichstein, M., Migliavacca, M., 2024. Interpretability of negative latent heat fluxes from eddy covariance measurements in dry conditions. Biogeosciences 21 (8), 2051–2085. https://doi.org/10.5194/bg-21-2051-2024.
Paulus, S.J., Migliavacca, M., Reichstein, M., Orth, R., Lee, S.-C., Carrara, A., Hildebrandt, A., Nelson, J.A., 2025. Insights into Water Vapor Uptake by Dry Soils using a Global Eddy Covariance Observation Network. Glob. Chang. Biol. 31 (10), e70547. https://doi.org/10.1111/gcb.70547.
Peters, A., Groh, J., Schrader, F., Durner, W., Vereecken, H., Pütz, T., 2017. Towards an unbiased filter routine to determine precipitation and evapotranspiration from high precision lysimeter measurements. J. Hydrol. 549, 731–740. https://doi.org/10.1016/j.jhydrol.2017.04.015.
Price, J., 2011. Radiation fog. Part I: Observations of Stability and drop size Distributions. Bound.-Lay. Meteorol. 139 (2), 167–191. https://doi.org/10.1007/s10546-010-9580-2.
Price, J., Clark, R., 2014. On the Measurement of Dewfall and Fog-Droplet Deposition. Bound.-Lay. Meteorol. 152 (3), 367–393. https://doi.org/10.1007/s10546-014-9930-6.
Pütz, T., Kiese, R., Wollschläger, U., Groh, J., Rupp, H., Zacharias, S., Priesack, E., Gerke, H.H., Gasche, R., Bens, O., Borg, E., Baessler, C., Kaiser, K., Herbrich, M., Munch, J.-C., Sommer, M., Vogel, H.-J., Vanderborght, J., Vereecken, H., 2016. TERENO-SOILCan: a lysimeter-network in Germany observing soil processes and plant diversity influenced by climate change. Environ. Earth Sci. 75 (18), 1–14. https://doi.org/10.1007/s12665-016-6031-5.
Resco de Dios, V., Chowdhury, F.I., Granda, E., Yao, Y., Tissue, D.T., 2019. Assessing the potential functions of nocturnal stomatal conductance in C3 and C4 plants. New Phytol. 223 (4), 1696–1706. https://doi.org/10.1111/nph.15881.
Ritter, F., Berkelhammer, M., Beysens, D., 2019. Dew frequency across the US from a network of in situ radiometers. Hydrol. Earth Syst. Sci. 23 (2), 1179–1197. https://doi.org/10.5194/hess-23-1179-2019.
Rothfuss, Y., Vereecken, H., Brüggemann, N., 2013. Monitoring water stable isotopic composition in soils using gas-permeable tubing and infrared laser absorption spectroscopy. Water Resour. Res. 49 (6), 3747–3755. https://doi.org/10.1002/wrcr.20311.
Runyan, C., Wang, L., Lawrence, D., D'Odorico, P., 2019. Ecohydrological Controls on the Deposition of Non-rainfall Water, N, and P to Dryland Ecosystems. In: D'Odorico, P., Porporato, A., Wilkinson Runyan, C. (Eds.), Dryland Ecohydrology. Springer International Publishing, Cham, pp. 121-137.
Saaltink, M.W., Kohfahl, C., Molano-Leno, L., 2020. Analysis of water vapor adsorption in soils by means of a lysimeter and numerical modeling. Vadose Zone J. 19 (1), e20012. https://doi.org/10.1002/vzj2.20012.
Schneider, J., Groh, J., Pütz, T., Helmig, R., Rothfuss, Y., Vereecken, H., Vanderborght, J., 2021. Prediction of soil evaporation measured with weighable lysimeters using the FAO Penman–Monteith method in combination with Richards' equation. Vadose Zone J. 20 (1), e20102. https://doi.org/10.1002/vzj2.20102.
Schnepper, T., Groh, J., Gerke, H.H., Reichert, B., Pütz, T., 2023. Evaluation of precipitation measurement methods using data from a precision lysimeter network. Hydrol. Earth Syst. Sci. 27 (17), 3265–3292. https://doi.org/10.5194/hess-27-3265-2023.
Schoppach, R., Claverie, E., Sadok, W., 2014. Genotype-dependent influence of night-time vapour pressure deficit on night-time transpiration and daytime gas exchange in wheat. Funct. Plant Biol. 41 (9), 963–971. https://doi.org/10.1071/FP14067.
Schrader, F., Durner, W., Fank, J., Gebler, S., Pütz, T., Hannes, M., Wollschläger, U., 2013. Estimating Precipitation and actual Evapotranspiration from Precision Lysimeter Measurements. Procedia Environ. Sci. 19, 543–552. https://doi.org/10.1016/j.proenv.2013.06.061.
Sibley, A., Schulze, M., Jones, J., Kennedy, A., Still, C., 2022. Canopy wetting patterns and the determinants of dry season dewfall in an old growth Douglas-fir canopy. Agric. For. Meteorol. 323, 109069. https://doi.org/10.1016/j.agrformet.2022.109069.
Simó, G., Martínez-Villagrasa, D., Jiménez, M.A., Caselles, V., Cuxart, J., 2018. Impact of the Surface–Atmosphere Variables on the Relation between Air and Land Surface Temperatures. Pure Appl. Geophys. 175 (11), 3939–3953. https://doi.org/10.1007/s00024-018-1930-x.
Sträter, E., Westbeld, A., Klemm, O., 2010. Pollution in coastal fog at Alto Patache, Northern Chile. Environ. Sci. Pollut. Res. 17 (9), 1563–1573. https://doi.org/10.1007/s11356-010-0343-x.
Sun, X., Amelung, W., Klumpp, E., Walk, J., Mörchen, R., Böhm, C., Moradi, G., May, S. M., Tamburini, F., Wang, Y., Bol, R., 2024. Fog controls biological cycling of soil phosphorus in the Coastal Cordillera of the Atacama Desert. Glob. Chang. Biol. 30 (1), e17068. https://doi.org/10.1111/gcb.17068.
Tall, A., Kandra, B., Pavelková, D., Reth, S., Gomboš, M., 2023. Evaluation of precipitation measurements using a standard rain gauge in relation to data from a precision lysimeter. Journal of Hydrology and Hydromechanics 71 (4), 413–424. https://doi.org/10.2478/johh-2023-0024.
Tardif, R., Rasmussen, R.M., 2008. Process-Oriented Analysis of Environmental Conditions Associated with Precipitation fog events in the New York City Region. J. Appl. Meteorol. Climatol. 47 (6), 1681–1703. https://doi.org/10.1175/2007JAMC1734.1.
Tian, C., Wang, L., Beysens, D., Kaseke, K.F., Medici, M.G., 2019. Isotopic investigation of dew origins and formation mechanisms under different climate conditions, 8th International Conference on Fog, Fog Collection and Dew. IFDA, Taipei, Taiwan.
Tian, C., Jiao, W., Beysens, D., Farai Kaseke, K., Medici, M.-G., Li, F., Wang, L., 2021. Investigating the role of evaporation in dew formation under different climates using 17O-excess. J. Hydrol. 592, 125847. https://doi.org/10.1016/j.jhydrol.2020.125847.
Tian, C., Du, K., Wang, L., Zhang, X., Li, F., Jiao, W., Beysens, D., Kaseke, K.F., Medici, M.-G., 2022. Stable isotope variations of dew under three different climates. Sci. Data 9 (1), 50. https://doi.org/10.1038/s41597-022-01151-6.
Uclés, O., Villagarcía, L., Cantón, Y., Domingo, F., 2016. Partitioning of non rainfall water input regulated by soil cover type. Catena 139, 265–270. https://doi.org/10.1016/j.catena.2015.02.018.
Urbaneja-Bernat, P., Tena, A., González-Cabrera, J., Rodriguez-Saona, C., 2020. Plant guttation provides nutrient-rich food for insects. Proc. R. Soc. B Biol. Sci. 287 (1935), 20201080. https://doi.org/10.1098/rspb.2020.1080.
Vargas Zeppetello, L.R., Trevino, A.M., Huybers, P., 2024. Disentangling contributions to past and future trends in US surface soil moisture. Nat. Water. https://doi.org/10.1038/s44221-024-00193-x.
Verhoef, A., Diaz-Espejo, A., Knight, J.R., Villagarcía, L., Fernández, J.E., 2006. Adsorption of Water Vapor by Bare Soil in an Olive Grove in Southern Spain. J. Hydrometeorol. 7 (5), 1011–1027. https://doi.org/10.1175/jhm556.1.
Wang, L., Kaseke, K.F., Seely, M.K., 2017. Effects of non-rainfall water inputs on ecosystem functions. Wiley Interdiscip. Rev. Water 4 (1), e1179-n/a. https://doi.org/10.1002/wat2.1179.
Weedon, G.P., Osborne, S.R., Best, M.J., 2024. Dew, frost, fog and lifted temperature minima: Observations in southern England and implications for modelling. Q. J. R. Meteorolog. Soc. https://doi.org/10.1002/qj.4702.
Wilson, T.B., Bland, W.L., Norman, J.M., 1999. Measurement and simulation of dew accumulation and drying in a potato canopy. Agric. For. Meteorol. 93 (2), 111–119. https://doi.org/10.1016/S0168-1923(98)00116-6.
Winkel, T., Lhomme, J.P., Laura, J.P.N., Alcón, C.M., del Castillo, C., Rocheteau, A., 2009. Assessing the protective effect of vertically heterogeneous canopies against radiative frost: the case of quinoa on the andean Altiplano. Agric. For. Meteorol. 149 (10), 1759–1768. https://doi.org/10.1016/j.agrformet.2009.06.005.
Wisniewski, J., 1982. The potential acidity associated with dews, frosts, and fogs. Water Air Soil Pollut. 17 (4), 361–377. https://doi.org/10.1007/BF00460104.
Xiao, H., Meissner, R., Seeger, J., Rupp, H., Borg, H., 2009. Effect of vegetation type and growth stage on dewfall, determined with high precision weighing lysimeters at a site in northern Germany. J. Hydrol. 377 (1–2), 43–49. https://doi.org/10.1016/j.jhydrol.2009.08.006.
Xie, J., Su, D., Lyu, S., Bu, H., Wo, Q., 2021. Dew formation characteristics of meadow plants canopy at different heights in Hulunbuir grassland, China. Hydrology Research, 10.2166/nh.2021.168.
Xu, Y., Jia, C., Liu, X., Zhao, Y., Dou, Y., Yang, X., Yi, Y., 2023. Monitoring the Dew Amount in typical Ecosystems of Northeast China from 2005 to 2021. Water 15 (6), 1091.
Yu, X., Huang, Y., Li, E., Li, X., Guo, W., 2018. Effects of rainfall and vegetation to soil water input and output processes in the Mu Us Sandy Land, northwest China. Catena 161, 96–103. https://doi.org/10.1016/j.catena.2017.10.023.

Zhang, Q., Wang, S., Yue, P., Wang, R., 2019a. A measurement, quantitative identification and estimation method(QINRW) of non-rainfall water component by lysimeter. MethodsX. https://doi.org/10.1016/j.mex.2019.11.012.
Zhang, Q., Wang, S., Yue, P., Wang, S., 2019b. Variation characteristics of non-rainfall water and its contribution to crop water requirements in China's summer monsoon transition zone. J. Hydrol. 578, 124039. https://doi.org/10.1016/j.jhydrol.2019.124039.
Zhuang, Y., Zhao, W., 2014. Dew variability in three habitats of a sand dune transect in a desert oasis ecotone, Northwestern China. Hydrol. Process. 28 (3), 1399–1408. https://doi.org/10.1002/hyp.9675.